Available online at www.sciencedirect.com
ScienceDirect
Bioorganic & Medicinal Chemistry Letters 17 (2007) 3445–3453
Bioorganic & Medicinal Chemistry Letters

Synthesis and structure–activity relationships of novel pyrimido[1,2-*b*]indazoles as potential anticancer agents against A-549 cell lines☆

T. Yakaiah,[a] B. P. V. Lingaiah,[a] B. Narsaiah,[a,*] B. Shireesha,[b] B. Ashok Kumar,[c] S. Gururaj,[d] T. Parthasarathy[c] and B. Sridhar[e]

[a]*Fluoroorganic Division, Indian Institute of Chemical Technology, Hyderabad 500 007, India*
[b]*College of Pharmaceutical Sciences, Kakatiya University, Warangal 506 302, India*
[c]*Department of Chemistry, Nizam College, Basheer Bagh, Hyderabad 500 001, India*
[d]*Global Institute of Biotechnology, Himayatnagar, Hyderabad 500 001, India*
[e]*Laboratory of X-ray Crystallography, Indian Institute of Chemical Technology, Hyderabad 500 007, India*

Received 7 November 2006; revised 5 March 2007; accepted 27 March 2007
Available online 30 March 2007

Abstract—A series of novel pyrimido[1,2-*b*]indazoles **5**, **7** have been prepared from 3-trifluoromethyl-5-phenyl-2,6-dicyano anilines **1** via novel indazole regioisomers **3** and **4** through a facile strategy. Specific examples were evaluated for anticancer activity in vitro and found to exhibit promising activity against A-549 cell lines and are more effective than Etoposide. QSAR models were developed and validated by cross-validation method. The results of the best QSAR model were further compared with the crystal structure of tubulin protein. The binding energies estimated were found to have a good correlation with the experimental inhibitory potencies.

The modern trend is directed towards discovery of new organic molecules as potential anticancer agents by adopting various synthetic approaches. In this process some of the molecules considered to interfere effectively with DNA either directly or inhibiting DNA–binding enzymes led to identification of new promising anticancer agents.[1] However, these molecules lack specificity towards cytotoxicity and damage cell lines in the tissue as a result no clear-cut drug is available. The principal driving force for stacking and charge transfer interactions is through hydrogen bonding and electrostatic forces.[2] In addition, strategically positioned suitable substituents promote interference with cellular detoxification pathways. Therefore, our attention was attracted towards synthesis of a series of novel pyrimido[1,2-*b*]indazoles with trifluoromethyl group at an appropriate position in order to identify suitable lead compounds as new pyrimido[1,2-*b*]indazoles as anticancer agents. Earlier findings have been on indazole derivatives specifically known to be active as protein kinase inhibitors, in cancer cell proliferative disorders, Alzheimer's disease, viral infections, auto-immune diseases and neuro degenerative disorders.[3–6] Further, pyrimidine ring in an organic molecule also shows prominent activity against several diseases.[7–9] Therefore interest is continuously increasing on fusion of pyrimidine ring over indazoles as a result pyrimido[1,2-*b*]indazoles are formed and are considered to have promising activity against many infections. Synthesis of pyrimido[1,2-*b*]indazoles is mainly starting from 3-amino indazoles and their reaction with 1,3-diketones,[10–12] β-ketoester,[13] propiolic acid ester,[14] DEEM[15] or DMAD.[16] In recent past, synthesis based on microwave irradiation conditions[17,18] is considered as a powerful synthetic tool due to its short reaction times, operational simplicity with improved yields and is of modern trend in organic synthesis. In continuation of our efforts[19–22] on the synthesis of novel ring systems of biological interest, we wish to report the synthesis of new indazole regioisomers **3**, **4** and each isomer is independently reacted with various substrates such as 1,3-diketones (symmetrical/unsymmetrical), diethyleth-

Keywords: Regioisomers; Indazoles; 1,3-Diketones; Pyrimido[1,2-*b*]indazoles; Cyclisation; A-549 cell lines; QSAR modelling studies; Tubuline.
☆ IICT Communication No. 041004.
* Corresponding author. Fax: +91 40 27160387x27193185; e-mail: narsaiah@iict.res.in

0960-894X/$ - see front matter © 2007 Elsevier Ltd. All rights reserved.
doi:10.1016/j.bmcl.2007.03.087

oxymethylene malonoate (DEEM), ethoxymethylene malononitrile (MMN), ethyl ethoxymethylene cyanoacetate (EMCA), diethyl *N*,*N*-dimethylaminomethylene malonate (DAMM), β-ketoesters and dimethyl acetylenedicarboxylate (DMAD) under microwave irradiation conditions obtaining pyrimido[1,2-*b*]indazoles **5**, **7** in high yields. Representative examples were screened for anticancer activity against A-549 cell lines and found to have more activity than Etoposide, a standard drug. Molecular modelling studies further confirmed the activity.

The 3-trifluoromethyl-5-phenyl-2,6-dicyano aniline **1** has three active functional groups ortho to each and is subjected to diazotisation using $NaNO_2$/HCl at 0 °C followed by potassium iodide obtaining corresponding iodobenzene **2**.[21] It is further reacted with hydrazine hydrate in refluxing ethanol resulting in two 3-amino-4/6-trifluoromethyl-6/4-phenyl indazole regioisomers **3**, **4** in definite proportions. The reaction is mainly nucleophilic substitution of iodine by hydrazine on benzene ring due to presence of powerful electron-withdrawing groups followed by selective attack on one of the nitrile carbons at a time to result in products **3**, **4**. The reaction is schematically drawn below in Scheme 1.

Each of indazole regioisomers **3** and **4** is separated due to their small difference in polarity and characterised based on IR, ^{1}H NMR, ^{13}C NMR, ^{19}F NMR (Table 1), mass spectral data and X-ray analysis. Compound **3** is less polar than compound **4** based on TLC and characteristic difference in chemical shifts of NH_2 group and proton on C-5 carbon is clearly observed in ^{1}H NMR. In compound **3**, NH_2 and C-5 proton signals appeared in upfield compared to compound **4** and it is assumed to be the influence of CF_3 and CN groups. If CF_3 and CN are para to each other, the electron-withdrawing effect in ring nullifies as a result the signals appeared in upfield as seen in compound **3**. In case CF_3 and CN are ortho to each, the cumulative electron-withdrawing effect enhances and with that, the signals for NH_2 and C-5 proton in ^{1}H NMR appeared in downfield in compound **4**. Further, phenyl protons appeared as singlet due to magnetic equivalence when CF_3 and CN are para to each other and multiplet if ortho to each other.

The ^{13}C NMR data of compounds **3** and **4** further support that the CF_3 carbon in compounds **3** appeared as quartet at δ 121.31 and in compound **4** as quartet at δ 122.76 with the same coupling constant 274 Hz. However, a characteristic difference of absorption of *C*-CF_3 is observed. In compound **3** the *C*-CF_3 appeared as quartet at δ 123.29 with coupling constant 31 Hz, whereas in compound **4** the *C*-CF_3 appeared as quartet at δ 130.16 with coupling constant 31 Hz. In addition nitrile carbon (CN) appeared at 126.99 for compound **3** and 113.16 for compound **4**. Thus, the structure of each isomer is determined. It is further confirmed by single crystal X-ray analysis of compound **3** and presented in Figure 1. CCDC 270847 contains supplementary crystallographic data for the structure **3** (see Figs. 2 and 3).

Reaction of compounds **3** *and* **4** *with 1,3-diketones.* The regioisomers **3** and **4** are independently reacted with 1,3-diketones (symmetrical and unsymmetrical) in a sealed tube under microwave irradiation conditions obtaining pyrimido[1,2-*b*]indazoles **5** in single step. The sequence of reaction is initially nucleophilic attack

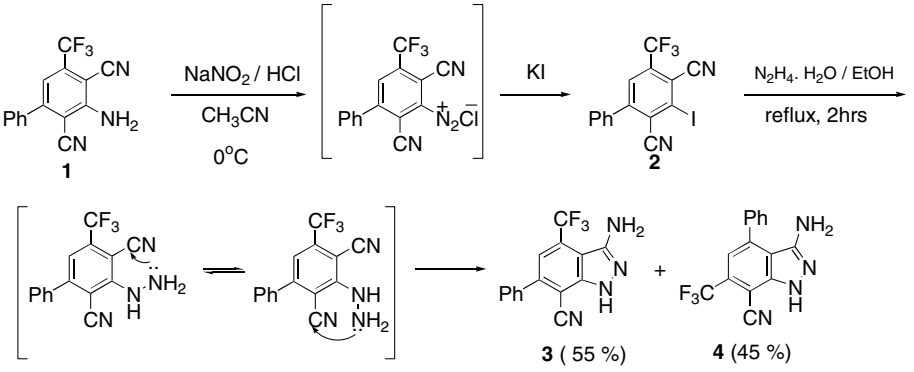

Scheme 1.

Table 1. ^{19}F NMR ($CDCl_3$) in ppm data for compounds **5d**, **5f** and **5k**, **5m**, **5n**

	3	4	5d	5f	5k	5m	5n
3-CF_3	—	—	58.78	58.46	—	—	—
4-CF_3	55.04	—	—	—	—	—	—
5-CF_3	—	—	—	—	60.90	61.10	58.07
6-CF_3	—	55.37	—	—	—	—	—
8-CF_3	—	—	66.43	66.95	—	—	—
10-CF_3	—	—	—	—	67.09	67.52	66.42

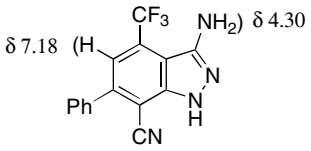

Chemical shift (up field)

Figure 1.

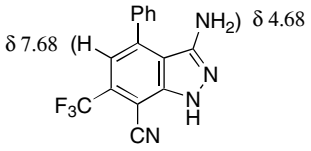

Chemical shift (down field)

Figure 2.

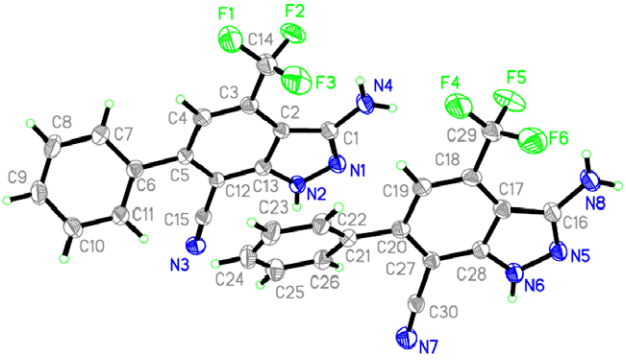

Figure 3. X-ray crystal structure of **3**. Displacement ellipsoids are drawn at 30% probability level and H atoms are shown as small spheres of arbitrary radii.

on one of the carbonyl carbons followed by cyclisation onto other carbonyl carbon to form products **5**. In case of reaction of unsymmetrical 1,3-diketones like 1,1,1-trifluoromethyl-2, 4-pentanedione, 1-phenyl-2, 4-butanedione, 4-phenyl-1, 1,1-trifluoro-2, 4-butanedione or 4-(4-methyl phenyl)-1,1,1-trifluoro-2, 4-butanedione with compounds **3/4** it resulted exclusively in one isomer **5d**, **5e**, **5f** or **5g/5k**, **5l**, **5m**, or **5n**, respectively. It is known[23,24] that the carbonyl attached to CF_3 group in 1,3-diketones is prone to enolise as a result the carbonyl remote from the CF_3 preferentially reacts first, gives exclusively one isomer and it is comparable with our earlier experience.[25] In addition, the mode of nucleophilic attack of regioisomers **3** and **4** on unsymmetrical 1,3-diketones is in two ways. In regioisomer **3** the primary amine is more reactive than tertiary nitrogen, whereas in regioisomer **4**, primary amine is less reactive than tertiary nitrogen. This is mainly due to their strategic position with respect to trifluoromethyl group in benzene ring. The reaction is schematically drawn below in Scheme 2.

In order to characterise a specific product from the reaction of unsymmetrical 1,3-diketones with regioisomers **3** and **4**, ^{19}F data are generated and tabulated in Table 1.

Reaction of compounds **3** *and* **4** *with DEEM/EMMN/EMCA/DAMM.* The compounds **3** and **4** are independently reacted with DEEM/EMMN/EMCA/DAMM in sealed tube under microwave irradiation conditions with 450 W power and obtained pyrimido[1,2-*b*]indazoles **7**. In case of DEEM and DAMM an uncyclised intermediate **6a** is formed from compound **3** and **6b** from

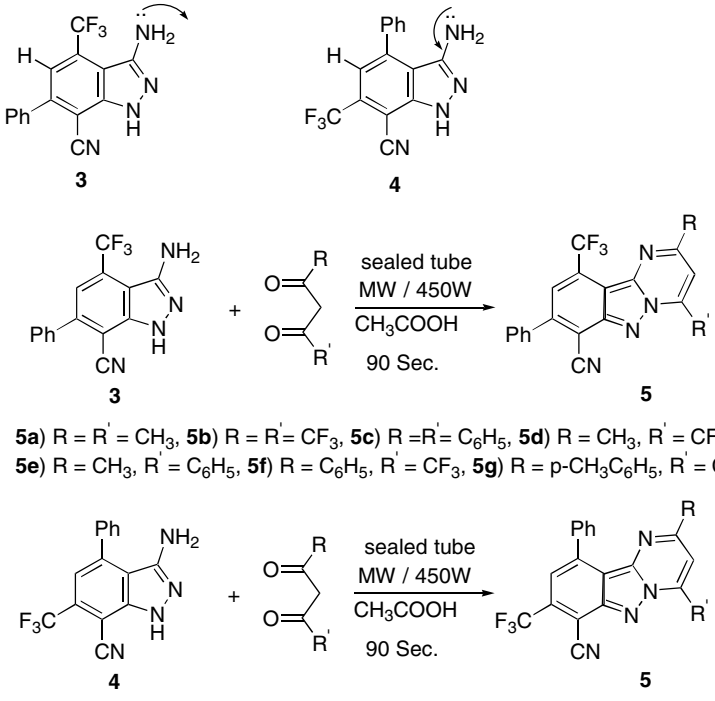

5a) R = R' = CH_3, **5b**) R = R'= CF_3, **5c**) R =R'= C_6H_5, **5d**) R = CH_3, R' = CF_3,
5e) R = CH_3, R' = C_6H_5, **5f**) R = C_6H_5, R' = CF_3, **5g**) R = p-$CH_3C_6H_5$, R' = CF_3.

5h) R = R' = CH_3, **5i**) R = R'= CF_3, **5j**) R =R' = C_6H_5, **5k**) R = CF_3, R' = CH_3,
5l) R = C_6H_5 ,R'= CH_3, **5m**) R = CF_3, R' = C_6H_5, **5n**) R = CF_3, R' = p-$CH_3C_6H_5$.

Scheme 2.

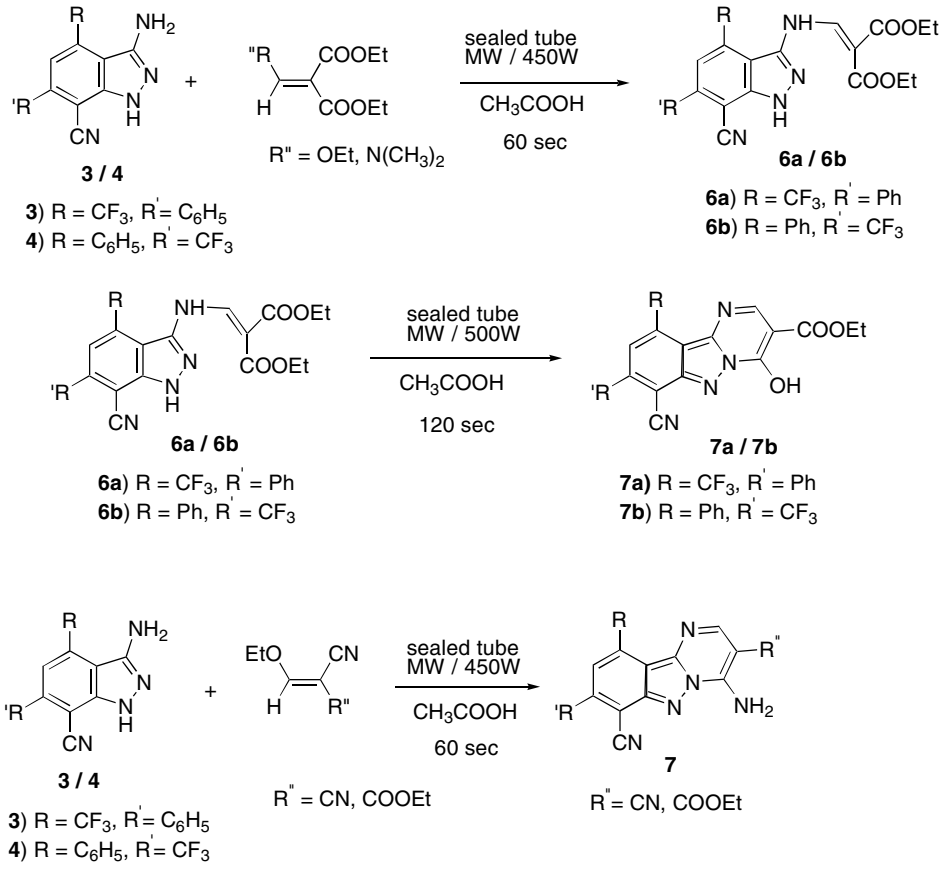

Scheme 3.

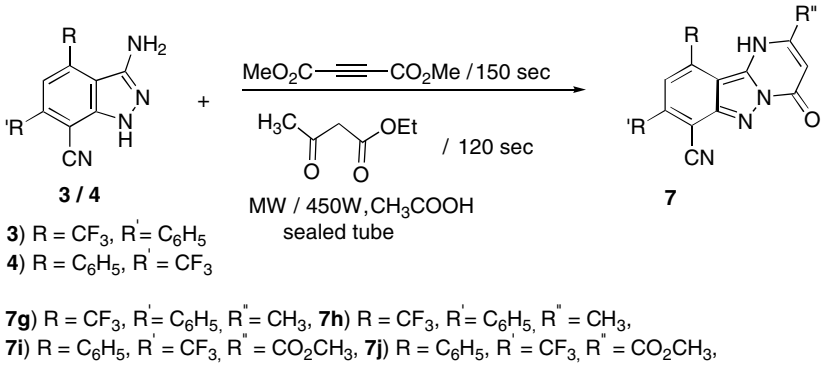

Scheme 4.

compound **4** which are further cyclised to give products **7a** and **7b** under microwave irradiation conditions with 450 W power, respectively. It is attributed to the nucleophilic nature of nitrile carbon (CN) versus ester carbonyl (CO_2Et) and ester carbonyl is considered to be sluggish. The ^1H NMR of compounds **7d** and **7f** is quite interesting in a way that the NH_2 protons in each of compounds appeared as two broad singlets with different chemical shifts. This is due to extended conjugation with ester carbonyl as a result proton became non-equivalent. The reaction is schematically drawn below in Scheme 3.

Reaction of compounds **3** *and* **4** *with* β*-ketoesters/DMAD.* The compounds **3** and **4** are similarly reacted with β-ketoesters/DMAD and respective products obtained. In case of β-ketoester the reaction is initiated by nucleophilic attack on carbonyl carbon followed by cyclisation, whereas with DMAD, the reaction is in addition followed by cyclisation. The reaction is schematically drawn below in Scheme 4.

Representative examples of pyrimido[1,2-*b*]indazole regioisomers with trifluoromethyl group at an appropriate position were synthesized and representative exam-

Table 2. Anticancer activity profile

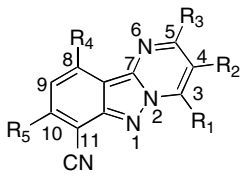

Compound	R_1	R_2	R_3	R_4	R_5	% inhibition[a]
7h	=O	H	CH_3	–Ph	CF_3	0.44
5a	CH_3	H	CH_3	CF_3	–Ph	3.74
5b	CF_3	H	CF_3	CF_3	–Ph	4.54
5l	CF_3	H	–Ph	–Ph	CF_3	4.80
5j	–Ph	H	–Ph	–Ph	CH_3	5.96
5k	CF_3	H	CF_3	–Ph	CF_3	6.44
5h	CH_3	H	CF_3	–Ph	CF_3	6.71
5n	CF_3	H	*p*-$CH_3C_6H_4$	–Ph	CF_3	6.77
7b	OH	COOEt	H	–Ph	CF_3	8.24
5m	CF_3	H	–Ph	–Ph	CF_3	8.90
5i	CF_3	H	CF_3	–Ph	CF_3	10.23
7d	NH_2	COOEt	H	CF_3	–Ph	10.70
7e	NH_2	COOEt	H	–Ph	CF_3	11.00
5e	CH_3	H	–Ph	CF_3	–Ph	13.33
5f	CF_3	H	–Ph	CF_3	–Ph	16.20
Std.	—	—	—	—	—	1.15

[a] All the pharmacological studies were performed in duplicate at 1 nM/ml (1 nM compound in 1 ml of 1% DMSO in PBS). % inhibition of cell growth is measured based on absorbance at 550 nm by transferring plate to plate reader. Std. Etoposide.

ples were evaluated for anticancer activity against A-549 cell lines by MTT assay method (Table 2).[26] The compound **5f** with trifluoromethyl group on C-3 carbon showed highest activity, whereas compound **7h** with hydroxyl group on C-3 carbon showed lowest activity. The compound inhibitory activity falls between 0.44% (**7h**) and 16.2% (**5f**). Based on the activity profile, it is broadly concluded that the presence of trifluoromethyl group in pyrimidine ring in combination of phenyl or additional trifluoromethyl group promotes high activity. Alternatively, the presence of activating groups like –OH, $–NH_2$ may also increase the activity as shown in compounds **7b**, **7d** and **7e**. However, the stability of the molecules is less due to the presence of ester group, which may prone to metabolize into acid. The activity data of these molecules are compared with those of Etoposide, a standard drug. Almost all the molecules showed greater inhibition than the standard Etoposide. The details of activity profile are tabulated in Table 2.

Cancer cell survival and viability in vitro were evaluated using the 3-(4,5-dimethylthiazol-2-yl)-2,5-diphenyltet-

Table 3. Activity and physicochemical parameters of indazole derivatives

Compound	Activity	log *P*	HOMO In ev	LUMO In ev	MR
5a	1.7282	4.4776	−9.58	−3.33	95.7375
5b	1.6440	6.7002	−8.49	−4.58	97.7579
5e	1.1762	6.3905	−8.92	−3.75	115.9102
5f	1.0915	7.5018	−8.69	−3.79	116.9204
5h	1.4743	5.5889	−9.07	−3.69	96.7477
5i	1.2912	6.7002	−8.47	−3.80	97.7579
5j	1.5258	7.8878	−8.75	−3.88	135.1504
5k	1.4921	6.7002	−8.83	−3.77	97.7579
5l	1.6198	6.3905	−3.33	−2.84	115.9102
5m	1.3516	7.5018	−8.7	−3.72	116.9204
5n	1.4704	7.9690	−8.69	−3.71	121.9616
7b	1.3851	5.0915	−9.23	−4.22	103.5715
7d	1.2716	4.5927	−9.20	−3.94	106.5778
7e	1.2596	4.5927	−9.17	−4.01	106.5778
[a]**7h**	2.6576	5.1115	−10.25	−3.69	93.7935
Std.	2.2403	2.6690		—	55.1636

[a]Considered as outlier.
Std. Etoposide.

Table 4. Model equations generated for the indazole analogues

Equation	Modelled Eq.	n	R	R^2	SEE	F
1	Act = −0.013(0.005)MR + 2.898(0.531) Q = 1.668; PRESS = 15.193; $q^2_{cv} = -0.089$	16	0.569	0.323	0.341	6.693
2	Act = −0.123(0.064)log P + 2.278(0.397) Q = 1.230; PRESS = 11.819; $q^2_{cv} = 0.152$	16	0.454	0.206	0.369	3.628
3	Act = 0.000137(0.000)MR^2 − 0.0392(0.033)MR + 4.103(1.575) Q = 1.730; PRESS = 15.193; $q^2_{cv} = 0.326$	16	0.597	0.356	0.345	3.597
4	Act = 0.013(0.040)log P^2 − 0.475(0.419)log P + 3.200(1.230) Q = 1.315; PRESS = 15.193; $q^2_{cv} = 0.343$	16	0.492	0.242	0.374	2.081
5	Act = 0.0578(0.022)log P^2 − 0.740(0.254)log P + 3.704(0.688) Q = 3.487; PRESS = 0.578; $q^2_{cv} = 0.527$	15	0.722	0.522	0.207	6.549
6	Act = 0.00024(0.000)MR^2 − 0.0563(0.016)MR + 4.649(0.789) Q = 4.795; PRESS = 0.358; $q^2_{cv} = 0.669$	15	0.820	0.672	0.171	12.300

n, number of data points; SEE, standard error estimate; Q, quality factor; PRESS, predictive sum of squares; q^2_{cv}, cross-validated.

razolium bromide (MTT, Sigma Chemical Co., St. Louis, MO) assay developed by Mosmann et al., with some modifications.

Test compounds are dissolved in 1 ml of DMSO. Cells were seeded in 96-well plate (10,000 cell/well) and left overnight in CO_2 incubator (at 5%) to recover from handling stress. Test compounds are added and incubated for 12 h. A 5 mg/ml MTT solution was prepared by dissolving in PBS (Phosphate buffer solution) and filter-sterilized. Added 20 µl of MTT solution from stock to each well containing cells and incubated the plate for another 5 h in a CO_2 incubator at 37 °C. Media were removed with needle and syringe. Added 200 µl of DMSO to each well to dissolve separated crystals of MTT. Kept the plate into incubator at 37 °C for 5 min. The % inhibition of cell growth is measured based on absorbance at 550 nm by transferring the plate-to-plate reader (This procedure is specific for adherent cells in 96-well plates.)

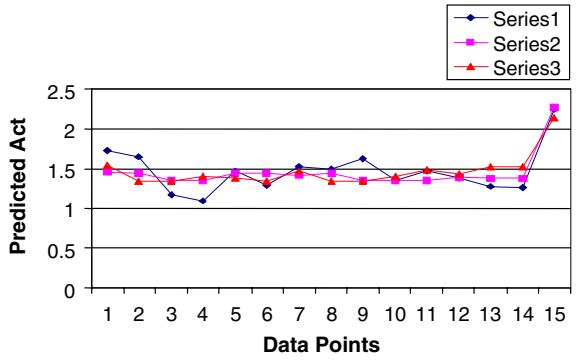

Figure 4. Comaparison of observed activity versus predicted activities. Series 1: observed activity; series 2: predicted activity (Eq. 5); series 3: predicted activity (Eq. 6).

With the aim of rationalizing the activity data obtained for the Indazole derivatives, a molecular modelling study was carried out in order to investigate the possible interaction of such compounds with tubulin protein. The stability of these molecules is derived from log P,[27] MR,[28] HOMO, LUMO values. Further QSAR studies were carried out on a series of indazole derivatives in order to provide further insight into the key structural features required to design potential drug candidates of this class. Molecular docking methodologies ultimately seek to predict the best mode by which a compound will fit into a binding site of a macromolecular target. In addition to the synthetic work, an attemptive explore of the QSAR and docking studies of indazole derivatives has been made to explain the observed variance in biological activity as a function of various molecular descriptors. This predicts the best drug candidate providing an insight into substitutional and configurational requirements for optimum receptor pit, which leads to the development of best pharmacophore activity.[29–31]

Docking was carried out against tubulin protein (pdb Code: **1SA1**), which is the possible anticancer target of indazole derivatives. Tubulin protein was chosen as a target for docking (using Openeye software,[32]) because of a relatively high tanimoto (2D structure finger print). Similarly index[33,34] of tubulin selected target protein was retrieved from Protein data bank.[35]

The activity data log (1/IC_{50}) and physicochemical properties log P, HOMO, LUMO and molar refractivity (MR) of the indazole derivatives are presented in Table 3. These data were subjected to regression analysis and the corresponding model equations were generated using SPSS 10.0 software[36] and are shown in Table 4.

Table 5. Docking functions and QSAR descriptors for analysis[32,36–38]

Descriptor code	Description
SG	Shapegauss (represents all the atoms as smooth Gaussian functions)-docking function score from Fred program
CG	ChemGauss (combines Shapegaussian function with additional potentials between chemically complimentary groups)-docking function score from Fred program
PLP	PLP (piecewise linear potential)-docking function score from Fred program
log P	Logarithm of partitioning coefficient (calculated by clog P method)
MR	Molar refractivity the measure of steric factor, bulkiness of the molecule

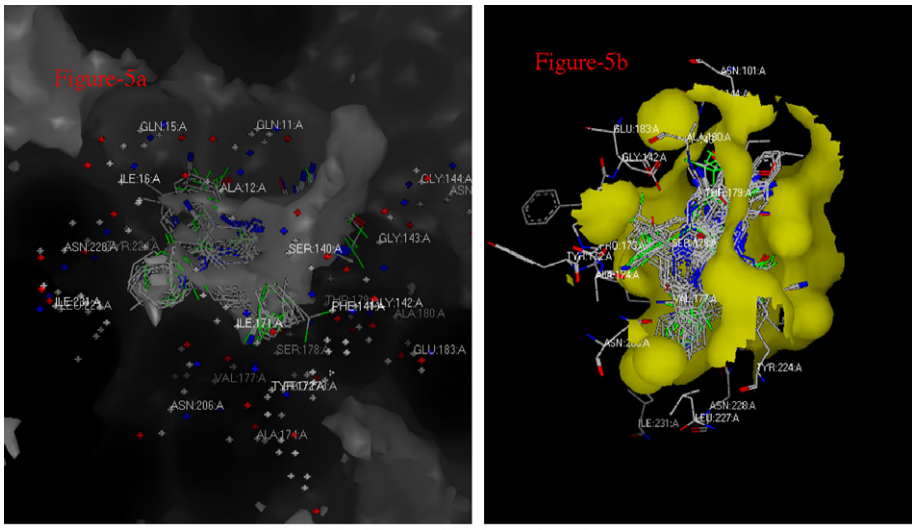

Figure 5. (a) Receptor cavity surface area. Amino acid in starmark. (b) Active site (amino acid) surface area.

Eqs. 1 and 2 show very lower correlation coefficients in terms of R^2 and Q values with respect to MR and log P, respectively. Further improvement, a quadratic term was included and Eqs. 3 and 4 were obtained which is statistically valid but with lower R and Q values (Table 4). Eqs. 5 and 6 (Table 4), which were resulted by taking an outlier (compound **7h**) on the basis of their residual values, show a high statistical significance.

The cross-validation parameters also reveal that Eqs. 5 and 6 were the best regression models having the higher value of Q, R^2, q^2_{cv} and low SEE values. From the graph (Fig. 4), a good agreement is observed by comparing the observed and predicted activities (derived from the best modelled equations) to the data points.

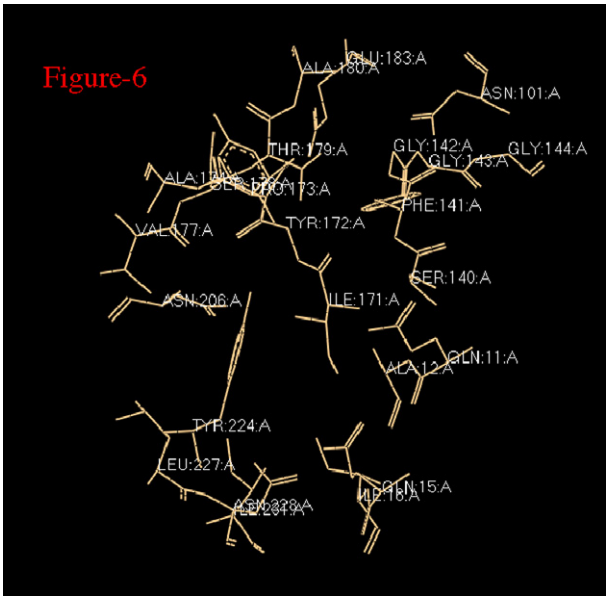

Figure 6. Active site region with amino acids.

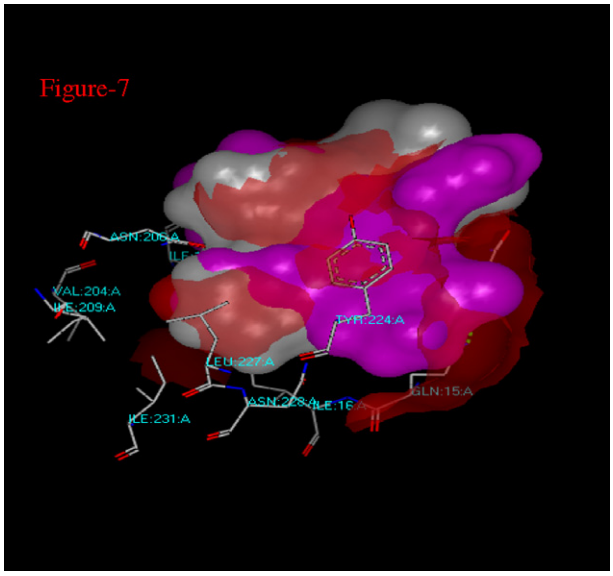

Figure 7. Compounds **5j** in purple and **5l** in grey colour representation in the active site region and their surface overlap.

Table 6. Scoring functions

Compound	Chemgauss	Clash	PLP	Screenscore	SHAPE
5a	−61.1	26.92	−40.25	−121.67	−471.23
5b	−67.57	26.82	−28.05	−116.68	−458.93
5e	−65.48	33.25	−26.42	−104.55	−501.99
5f	−74.19	35.03	−32.12	−124.1	−523.52
5h	−62.82	35.77	−28.51	−113.74	−432.53
5i	−61.3	56.15	3.88	−57.54	−432.7
5j	−67.84	69.50	−17.56	−100.12	−476.65
5k	−69.25	37.66	−17.2	−112.05	−470.01
5l	−74.56	43.69	−33.84	−136.13	−524.37
5m	−72.74	60.24	17.11	−55.41	−511.69
5n	−75.27	60.46	2.16	−83.41	−519.31
7b	−61.26	30.66	−32.88	−112.25	−465.73
7d	−71.86	29.57	−48.03	−129.65	−537.06
7e	−63.21	30.07	−30.66	−108.99	−459.5
7h	−63.64	44.84	−41.95	−127.14	−448.56
Std.	−40.19	21.52	−32.64	−90.06	−284.26

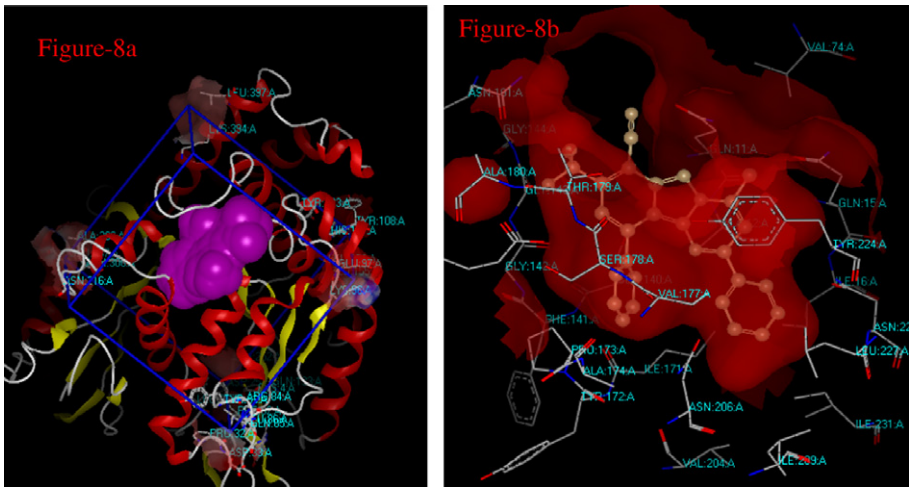

Figure 8. (a) 4 Å grid model along with the best molecular surface area (**5l**) in pink colour, protein in ribbon model. (b) Ball and stick model of the best molecule (**5l**) in the receptor pocket. Surface area of the receptor pocket is in red colour.

Since these are second-degree equations in log P and MR, an optimum log P and MR that corresponds to give maximum activity can be evaluated by finding the maxima. Eqs. 5 and 6 were partially differentiated with respect to log P and MR, respectively, the first derivative was set to zero and a value of $\log P_{opt} = 6.401$ and $MR_{opt} = 116.66$ was obtained. Therefore, the analogue with around 6.401 value of log P and around 116.66 value of MR is expected to show maximum activity.

Docking functions[37–39] and QSAR descriptors for analysis are given in Table 5. The predicted binding energies of Indazole analogues have shown good correlation with the respective inhibitory activities, that is, **5l** has lowest scoring values and higher inhibitory activity than standard reference molecule (std) and other analogues.

To visualize the binding conformations of these analogues within the active site of tubulin protein are displayed in Figure 5. In the active site region (4 Å) the tubulin protein nine amino acids that can play an important role are shown in Figure 4 (viz., Gln 11, Ala 12, Glu 71, Ser 140, Gly 142, Thr 145, Val 177, Asn 206 and Asn 228). As observed in Figure 5, **5l** and **5j** were docked in the active site of protein with a significant different binding mode compared with standard molecule (see Figs. 6 and 7).

Furthermore, differences in the binding mode were observed for **5l** and **5j** because of the presence of three phenyl groups in **5j**, increases in the bulkiness of the ligand resulting in highest clash penalty with the active site of the receptor amino acid (AA) (Table 6). Large substitution at R_1 position of indazole analogues may lead to collision with the residues Ser 178, Thr 179 and Ala 180 in the receptor site.

To further validate the binding mode best scored molecule in the grid as well as surface form is given in Figure 8.

In conclusion, the indazole regioisomers are prepared by convenient route and are considered as active synthons for building up of additional ring onto indazoles. Thus, it is demonstrated that pyrimidine ring can be fused onto indazoles with a variety of substrates and obtained pyrimido[1,2-*b*]indazoles under microwave irradiation conditions. A set of novel indazole derivatives have been synthesized and screened for anticancer activity by MTT assay method against A-549 cell lines. All the molecules showed higher activity than the standard Etoposide. The optimum lipophilic and bulkiness requirements are important to fit in the active site of the target and to have more hydrophobic affinity. The drug candidate with optimum value of log P (6.401) and MR (116.66) shows high activity. QSAR analysis and molecular docking studies were compared for the investigated compounds. The binding energies estimated by scoring functions were found to have a good correlation with the experimental inhibitory potencies. Based on the binding conformations from molecular docking, it is concluded that the presence of bulkier substituent (Ph) at R_3 position, in combination of CF_3 group in pyrimidine ring, promotes high activity.

Acknowledgments

The authors are thankful to Dr. J.S. Yadav, Director, IICT, and Shri S. Narayan Reddy, Head, Fluoroorganic division, IICT, Hyderabad, for their constant encouragement and financial support from industry-sponsored project. The author is thankful to the Head, Department of Chemistry, Nizam College, for providing the facilities for the work. We also thank Director Dr. N.V. Naidu (Global Institute of Biotechnology, Himayatnagar, Hyderabad) for providing the Software to complete the work.

References and notes

1. Rahman, A. U.; Malik, S. *Tetrahedron Lett.* **1985**, *26*, 2759.

2. Rahman, A. U.; Malik, S.; Sadiq, H. S.; Iqbal, C. M.; Chao-zhou, N.; Jon, C.; Nigellidine, F. *Tetrahedron Lett.* **1995**, *36*, 1993.
3. Conception, N.; Patrick, M.; Thompson, F.; Fabienne, M. T.; Eric, B.; Sylvie, W.; Cecile, C. PCT Int. Appl. WO 03 11, 833, **2003**, 188 pp. (Fr) (C.A. 138: 153529x).
4. Amici, R. D.; Matteo A. K. M.; Barbara S.; Anna Vetti. PCT Int. Appl. WO 03 28, 720, **2003**, 132 pp. (Eng) (C.A. 138: 304278t).
5. Renhowe, P. A.; Shafer, C. M.; McBridge, C.; Silver, J.; Pecchi, S.; Machajewski, T.; Mccrea, B.; Poon, D.; Thomas, T. PCT Int. Appl. WO 03 4, 488, **2003**, US (C.A. 138: 106699t).
6. Molina, P.; Arques, A.; Victoria, M.; Vinader, V. *Tetrahedron Lett.* **1989**, *30*, 6237.
7. Griffin, R. J.; Lowe, P. R. *J. Chem. Soc. Perkin Trans.* **1992**, *1*, 1811.
8. Whilock, B. J.; Lipton, S. H.; Strong, F. M. *J. Org. Chem.* **1965**, 115.
9. Schwan, T. J.; Howard Tieckemann, J. *J. Med. Chem.* **1965**, 750.
10. Domergue, A.; Sureau, F.; Robert, F. M.; Georges, A. (Ugine kuhlmann). Fr. 2, 192, 559, Appl. 72, 25, 693, **1974**, 7 pp (C.A. 81: 152260V).
11. Yu, V. M.; Chuiduk, V. A. *Khim. Geterotsikl, Soedin* **1974**, 984 (CA: 81. 120560b).
12. Chuiguk, V. A.; Gladkaya, V. A. *Ukr Khim. Zh. (Russ. Ed)*. **1981**, *47*, 966 (C.A. 97: 23724f).
13. Salvatore, P. V. S.; Marino, L. M. J. *Heteroatom Chem.* **1973**, *10*, 261.
14. Hans, R.; Peiren, M. A.; Roert, M. *Chem. Ber.* **1972**, *105*, 794.
15. Dong, L. H. P.; Claude, C. *Ger. Offen.* **1978**, *2*, 822, 124. (C.A. 90: 152181f).
16. Polanc, S.; Vestn, C.; Slov, C. *Kem. Drug.* **1984**, *31*, 115 (CA: 101. 191831h).
17. (a) Abramovitch, R. A. *Org. Prep. Proced. Int.* **1991**, *23*, 683; (b) Caddick, S. *Tetrahedron* **1995**, *51*, 10403; (c) Loupy, A.; Petit, A.; Hamelin, J.; Texier-Boultet, F.; Jacquault, P.; Mathe, D. *Synthesis* **1998**, 1213; (d) Varma, R. S. *Green Chem.* **1999**, *1*, 43.
18. (a) Yadav, J. S.; Reddy, B. V. S. *Tetrahedron Lett.* **2002**, *43*, 1905; (b) Yadav, J. S.; Reddy, B. V. S.; Madan, Ch.; Kumar, G. M. *Synlett* **2001**, 1781; (c) Yadav, J. S.; Reddy, B. V. S.; Rasheed, M. A.; Kumar, H. M. S. *Synlett* **2000**, 487; (d) Yadav, J. S.; Reddy, B. V. S. *New J. Chem.* **2000**, *24*, 489.
19. Venkat Reddy, G.; Rama Rao, V. V. V. N. S.; Maitraie, D.; Ravikanth, S.; Yadla, R.; Reddy, S. N.; Narsaiah, B.; Shanthan Rao, P. *J. Fluorine Chem.* **2003**, *124*, 203.
20. Rama Rao, V. V. V. N. S.; Venkat Reddy, G.; Maitraie, D.; Ravikanth, S.; Yadla, R.; Narsaiah, B.; Shanthan Rao, P. *Tetrahedron* **2004**, *60*, 12231.
21. Maitraie, D.; Venkat Reddy, G.; Rama Rao, V. V. V. N. S.; Ravikanth, S.; Narsaiah, B.; Shanthan Rao, P.; Ravikumar, K.; Sridhar, B. *Tetrahedron* **2005**, *61*, 3999.
22. Ravikanth, S.; Venkat Reddy, G.; Maitraie, D.; Rama Rao, V. V. V. N. S.; Shanthan Rao, P.; Narsaiah, B. *Syn. Commun.* **2004**, *34*, 4463.
23. Singh, S. P.; Kapoor, J. K.; Kumar, D.; Threadgil, M. D. *J. Fluorine Chem.* **1997**, *83*, 73.
24. Joseph, P. K.; Shanmugasundaram, P.; Ramakrishnan, V. T. *Indian J. Chem.* **1992**, *31*, 563.
25. Krishnaiah, A.; Narsaiah, B. *J. Fluorine Chem.* **2001**, *109*, 183.
26. Mosmann, T. *J. Immunol. Methods* **1983**, *65*, 55.
27. Bodor, N.; Buchwald, P. *J. Phys. Chem. B* **1997**, *101*, 3404.
28. Viswanadhan, V. N.; Ghose, A. K.; Revankar, G. R.; Robins, R. K. *J. Chem. Inf. Comput. Sci.* **1989**, *29*, 163.
29. Rameshwar, N.; Krishna, K.; Ashok Kumar, B.; Parthasarathy, T. *Bioorg. Med. Chem.* **2006**, *14*, 319.
30. Ravi, K. A.; Ashok, K. B.; Parthasarathy, T.; Uma, V. *Bioorg. Med. Chem.* **2005**, *13*, 1873.
31. Sirisha, M. A.; Ashok, K. B.; Parthasarathy, T.; Uma, V. *Centl. Eur. J. Chem.* **2004**, *4*, 696.
32. Fred 2.1, Omega 2.0, Openeye Scientific Software, Inc., 3600 Cerrillos Road, Suite 1107, Santa Fe, NM 87507, USA. www.eyesopen.com.
33. J. Chem., ChemAxon, ChemAxon Ltd, Maramaros koz 3/a, Budapest 1037, Hungary.
34. Willett, P.; Barnard, J. M.; Downs, G. M. *J. Chem. Inf. Comput. Sci.* **1998**, *38*, 983.
35. www.rcsb.org\pdb.
36. McGann, M. R.; Almond, H. R.; Nicholls, A.; Grant, J. A.; Brown, F. K. *Biopolymers* **2003**, *68*, 76.
37. Stahl, M.; Rarey, M. *J. Med. Chem.* **2001**, *44*, 1035.
38. Gehlhaar, D. K.; Verkhivker, G. M.; Rejto, P. A.; Sherman, C. J.; Fogel, D. B.; Fogel, L. J.; Freer, S. T. *Chem. Biol.* **1995**, *2*, 317.
39. SPSS software. Consult http://www.spss.com.